High fidelity DNA replication and repair: new structures and mechanisms using cryogenic electron microscopy

Borsellini, A.

Citation

Borsellini, A. (2022, October 19). *High fidelity DNA replication and repair: new structures and mechanisms using cryogenic electron microscopy*. Retrieved from https://hdl.handle.net/1887/3483673

An air-blades based plunge freezer for improved cryo-EM grid preparation

Alessandro Borsellini[1,3], Rafael F. Leiro[2,3], Leoni Abendstein[1], and Meindert H. Lamers[1]

[1]Department of Cell and Chemical Biology, Leiden University Medical Center, Leiden, The Netherlands. [2]Spanish National Cancer Research Centre (CNIO), Melchor Fernández Almagro 3, Madrid, Spain. [3] Contributed equally to this work.

Correspondence should be addressed to rfleiro@cnio.es and m.h.lamers@lumc.nl

Abstract

Cryogenic electron microscopy is a technique used to determine high resolution structures of biological macromolecules. A requirement for the success of this technique is the generation of thin layers of vitreous ice on the cryo-EM grid with heterogeneously distributed and randomly oriented particles. Although an increasingly high number of structures have been determined in the recent years with cryo-EM, there are occasions in which standard sample preparation methods are the limiting factor for the achievement of high-resolution structures. Here, we present a novel technique for improved cryo-EM grid preparation that is based on the use of two streams of gas for the generation of thin layers of protein solutions on the grid. In addition to this, the new plunge freezer described here allows the rapid mixing and vitrification of two solutions in millisecond time scale to perform time-resolved cryo-EM experiments.

Introduction

Cryo electron microscopy has become a powerful technique able to deliver high resolution structures of biological macromolecules with relatively easy sample preparation. As the hardware and software to perform cryo-EM have become more reliable, the success of this technique is increasingly dependent on the quality of the sample introduced into the microscope. The standard methodology for preparing cryo-EM samples relies on filter paper to blot away excess liquid from the cryo-EM grid, and plunge the grid into liquid ethane at ~ -182 degrees. In this process called plunge freezing, the particles ideally are evenly distributed and randomly oriented into a thin layer of vitrified liquid [1]. However, different problems can arise when preparing the sample with this technique. First, for some samples it can be difficult to obtain a thin layer of vitreous water suitable for high resolution imaging [2,3]. In addition, problems such as preferred orientation, aggregation, adverse interactions with the air water interface or with the filter paper can take place that compromise the quality of the data [4,5,6,7,8,9]. Hence, a time-consuming optimization may be required in order to obtain a grid that produces a high-resolution structure.

To overcome some of the problems associated with the blotting-paper based sample preparation, different techniques have been developed in recent years that improve the reproducibility of grid preparation, such as pin printing thin layers of sample on the grids [10,11], or spotting small drops of sample on self-wicking grids [5,12,13,5]. Other alternatives focused on development of time-resolved cryo-EM plunge freezers that can rapidly mix and spray small droplets onto holey carbon or self-wicking grids [14,15,16,17].

Here we present an inexpensive and easy to use blotting paper-free plunge freezer termed the "Puffalot" that can apply the sample, remove the excess of liquid and freeze the cryo-EM grid in a time window of 100-200 milliseconds. This new approach distinguishes itself from other techniques by a stream of pressurized gas (a "puff") that removes the

excess sample and produces thin layers of vitreous ice suitable for cryo-EM imaging, in a consistent and reproducible manner. Moreover, it allows the rapid mixing of two solution to perform time resolved cryo-EM studies on transient molecular states or transient interactions of macromolecules.

Results

Blotting-free plunge freezing using the Puffalot

The design and mode of operation of the Puffalot are illustrated in Figure 1 and Supplementary information. The grid is held between the tweezers tips as in standard plunge freezers (I). Two Hamilton syringes (II) containing 2-3 μL of sample each are pointing to the cryo-EM grid. Two solenoid pistons (III) on the back of the syringes push the sample onto the grid. Two pressurized gas nozzles (IV) generate a laminar flow of gas (the 'puff') that is parallel to the cryo-EM grid, and removes the excess of sample generating
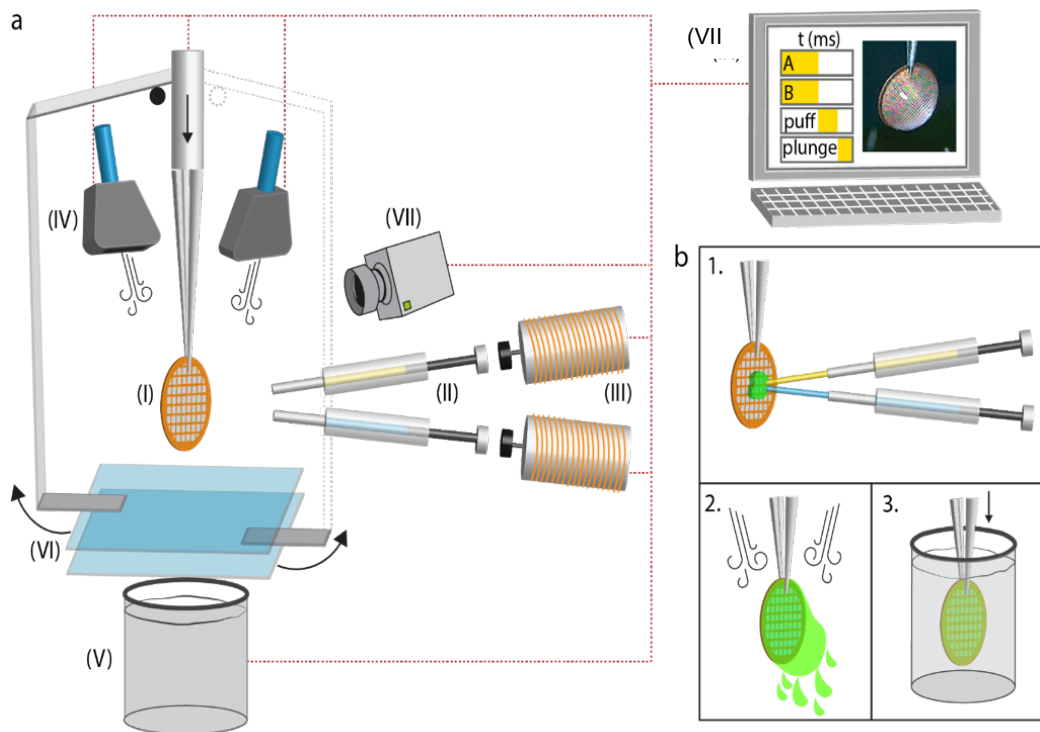

Figure 1 | Puffalot overview. a, Schematic representation of the Puffalot: (I) cryo-EM grid; (II) Hamilton syringes containing the sample; (III) Solenoid pistons; (IV) Gas nozzles; (V) Temperature controlled liquid ethane bath; (VI) Plastic shields that protect the ethane from the stream of gas; (VII) High speed camera; (VIII) Computer with software to regulate the plunge freezing timing. **b**, Schematic representation of the puffing-plunge freezing procedure: (1) Sample application; (2) Puff to remove the excess of solution; (3) Plunge freezing in liquid ethane.

a thin layer of liquid sample. The grid is then plunged into a temperature controlled liquid ethane bath, cooled to -182 °C (V). Two plastic shields (VI) are positioned on top of the liquid ethane to protect it from the puff of gas. The opening of these shields is simultaneous with the plunging of the grid into the liquid ethane. A high-speed camera (VII) is used to record slow motion videos (520 frames per second) while preparing the cryo-EM grid. This way it is possible to track the correct sample application on the grid. The electronic inputs that initiate all the procedures of sample application, puff, and plunge are controlled by a computer with in-house developed software (VIII). All together, the whole procedure can be as fast as 170 ms.

High resolution structures obtained from Puffalot grids

First, we tested the ability of the Puffalot to generate grids with suitable ice for cryo-EM studies by varying plasma treatment time, puff time and puff pressure. Unlike blot-based plunge freezing techniques, only five seconds of plasma treatment are needed in order to enable the removal of excess sample from the grid. The parameters that regulate the puff are important for the ice thickness. We observed that a blow of pressurised gas at 7 bar of a duration of 50 to 100 ms generates grids with many squares presenting thin ice (Fig. 2c-g). Shorter or longer puff time generate grids that are too thick or empty, respectively (Supplementary Figure 1). The ice thickness of the grids made with the Puffalot is not influenced by the protein sample or buffer components as shown by multiple proteins and buffers that have been tested, and all show squares with thin ice and well visible individual particles. Tomographic analysis of the ice shows that on average the grids prepared with the Puffalot contain squares with ice thickness in the range of 30 to 80 nm, which is optimal for SPA high resolution structure determination.

Next, we tested the ability of the Puffalot to generate grids of good quality for high-resolution cryo-EM structure determination. In order to do so, we collected a dataset on human Apoferritin, which resulted in a map with a resolution of 1.8 Å (Fig. 2). Details on data acquisition parameters are in Table 1. Comparison with results obtained on the same sample prepared with blot-paper based plunge freezers, demonstrates that the Puffalot consistently produces cryo-EM grids for suitable for high resolution structure determination.

Improving particle orientational distribution

The interaction between proteins and the air-water interface is often the factor that induces preferred orientations, and therefore limits the resolution of protein structures [18]. Calculations based on the diffusion constant of proteins demonstrate that the mean distance travelled by average size proteins (100-500 Å diameter) in 1 second is ~ 0.6 to 6 μm, which
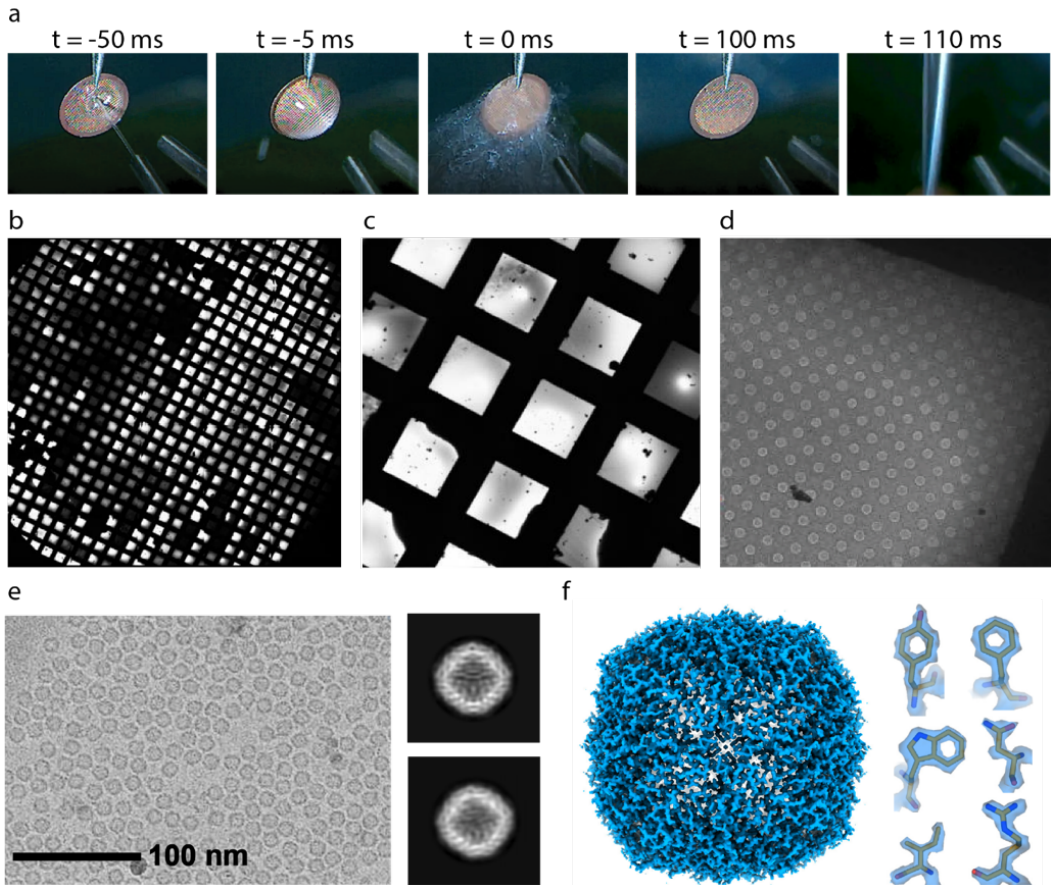
Figure 2 | Grid preparation and structure determination using the Puffalot. a, Time line of the Puffalot grid preparation procedure. At time -50 ms the sample is injected on the grid. Time zero is indicated as the initial moment of the "Puff". After 110 ms the grid is plunged in liquid ethane. **b**, representative grid. **c**, zoom in of grid squares from panel (b). **d**, zoom in of panel (c) showing holes with suitable ice for SPA cryo-EM. **e**, representative micrograph and 2D classes from apoferritin dataset. **f**, apoferritin density map at 1.8 Å resolution with detail of model fit to map.

is larger than the 0.1 μm liquid layers achieved during cryo-EM sample preparation (Supplementary material). This means that multiple times during plunge freezing proteins can interact and get trapped at the air-water interface. Results obtained from fast plunge freezers demonstrated that when the plunge freezing time is reduced to 6 - 200 ms the orientation distribution of proteins in the ice is more heterogeneous [19,5,16]. These time scales are still not small enough to prevent all the interaction with the air-water interface. However, the increased angular distribution of particles suggests that after the interaction with the air water interface, a second process takes place in which the particles explore their energy landscape before reaching local energy minimum [19]. Hence, plunge freezing
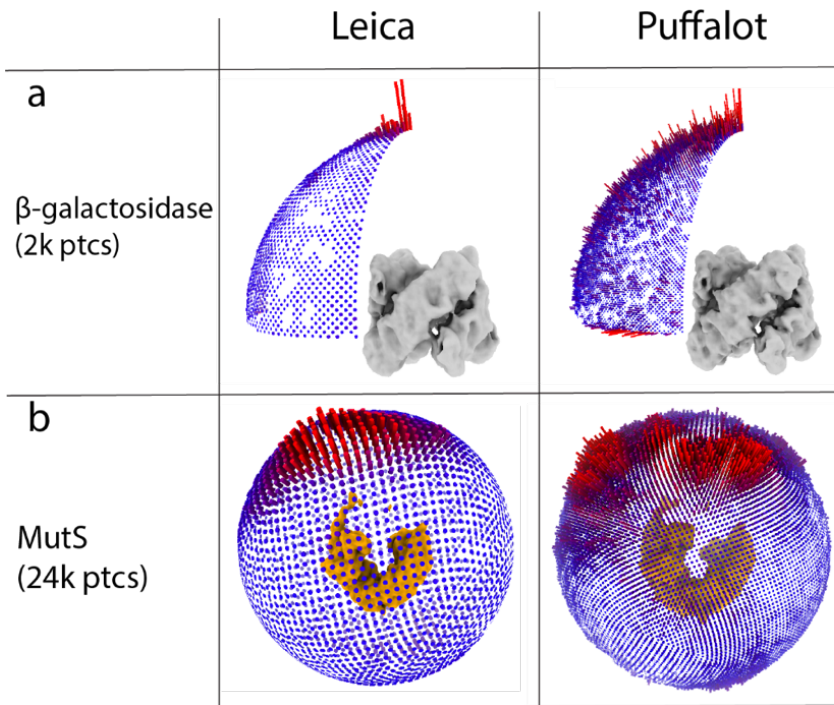
Figure 3 | Improved orientational distribution using the Puffalot. Density map and particle orientational distribution of (**a**) β-galactosidase from *T. maritima* and (**b**) MutS from *E. coli*, obtained preparing sample with the Leica plunge freezer (left) or with the Puffalot (right).

samples in the millisecond time scale seems to help in achieving a more heterogeneous set of particle orientations at the air-water interface.

In order to evaluate whether plunge freezing with the Puffalot helps in solving the problem of preferred orientation, we analysed samples which have been shown to strongly interact with the air-water interface. The proteins used are MutS form *Escherichia coli* (190 kDa), β-galactosidase from *Thermotoga maritima* (130 kDa). We prepared the specimens side-by-side on the Puffalot and on a Leica GP2 plunge freezer and performed single particle analysis to assess the differences in orientational distribution. Importantly, during sample preparation no detergents such as tween-20 were added to the buffers that could mask the effect of this plunge freezing technique in improving sample angular distribution. Details on data acquisition parameters are in Table 1. In order to properly analyse the pairs of datasets we randomly selected an equal number of particles at the end of the processing and used them for the final 3D reconstructions and angular assignment. All the specimens have a preferred orientation in the vitreous water layer (Fig. 3a). However, the reconstructions obtained from grids prepared with the Puffalot show a broader angular sampling and a reduced number of missing views, which is a prerequisite to obtain interpretable cryo-EM density maps.

Time resolved Cryo EM

The Puffalot furthermore offers the possibility to rapidly mix two solutions prior to vitrification. The two solutions can be placed in the two syringes, and mixed directly on the cryo-EM grid, before the puff of gas that removes the excess of liquid. First, we measured the efficient mixing of the solutions by loading Bradford protein stain in one syringe and a protein solution in the other syringe, and we followed the mixing of the two on the cryo-EM grid using the high-speed camera. As shown in Fig. 4a, the brown Bradford solution turns blue once the protein solution is applied to the cryo-EM grid, indicative of an efficient mixing of the two liquids.

Next, we used the Puffalot to look at the conformational change of the MutS protein, in response to ATP binding. It has been shown by stopped-flow assays that nucleotide binding into the ATPase domains of the MutS protein leads to a conformational change that can be followed by Förster resonance energy transfer (FRET) (Fig. 4b) [20]. The
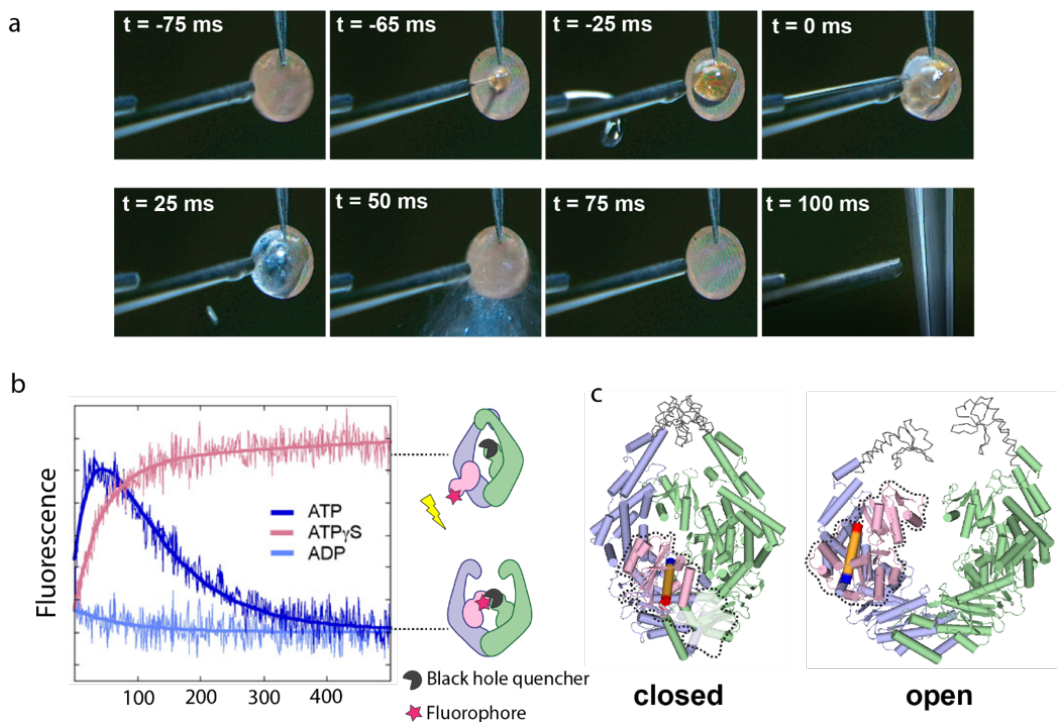

Figure 4 | Time resolved cryo-EM. a, Bradford protein stain (brown) and protein solution (transparent) mixing on the grid and change colour to blue, followed by the puffing-plunge freezing steps. **b**, Stopped-flow traces of MutS_IAANS mixed with various nucleotides show increase in fluorescence with ATPγS, slight decrease with ADP and biphasic increase and decrease with ATP (figure taken from Sharma A. *et al* 2013 [20]). On the right side of the graph, cartoon representation of pre-hydrolysis closed (top) and post hydrolysis open (bottom) conformations. Purple star and dark grey figure represent IAANS fluorophore and black hole quencher, respectively. **c**, cryo-EM structures of the closed and open MutS conformation.

conformational change is transient, as in less than 200 ms the ATP is hydrolysed and the protein returns to its original state. In contrast, the conformational change is retained when MutS is mixed with a non-hydrolysable ATP analogue (Fig. 4b). Consequently, when using a conventional blot-based plunger where several seconds pass between mixing of MutS and ATP and freezing, we observe the post-hydrolysis states of MutS when using ATP, and a closed, pre-hydrolysis state when using the non-hydrolysable ATP analogue AMPPNP [21]. In contrast, when we use the Puffalot to rapidly mix and freeze MutS and ATP, we observe a closed, pre-hydrolysis structure. Hence, the speed at which the Puffalot mixes and freezes samples will enable the investigation of transient conformational changes or transient interactions between macromolecules that were previously only attainable with mutants or non-hydrolysable substrates.

Discussion

Cryo-EM has become an essential technique for determination of protein structures due to the unique advantage of imaging proteins in their native conformations in vitrified aqueous solutions. However, it is not always easy to obtain thin layers of vitreous water with homogeneously distributed and properly folded proteins, which is a requirement to obtain suitable data for high resolution structure determination.

The main drawback of embedding proteins samples in vitreous water layers is the presence of two air-water interfaces, that have been shown to be surfaces of adsorption for the proteins in solution. Although many proteins are not affected by this phenomena, the adsorption on the air-water interface often causes problems such as preferred orientation, denaturation and multi protein complexes dissociation, that ultimately make the achievement of 3D structures impossible. Experiments performed by Klebl et al. [19] and Noble *et al.* [5] demonstrated that proteins that get denatured or adopt a preferred orientation at the air-water interface, benefit from faster vitrification procedures that happen in less than 200 ms.

Here we report the results obtained with the Puffalot, a new plunge freezer that can vitrify cryo-EM samples in a time range of 100-200 ms. In agreement with other fast instruments [19,5], fast plunge freezing with the Puffalot generates grids that display a broader angular distribution of proteins that show preferred orientations in grids prepared with blot-based plungers. Together with the fast plunge freezing capabilities, the Puffalot has several other attractive qualities: first, the whole grid surface is covered by the protein solution when the sample is injected on the grid. The puff of gas that removes the excess of buffer produces thin layers of ice in multiple grid squares, important when a high number of particles is needed to obtain a high-resolution structure. Second, the ice thickness is controlled by the puff time or strength and is independent of the protein and buffer used.

An additional advantage of the Puffalot is the rapid mix and plunge freezing capabilities, that can be used to trap intermediate states in proteins that adopt multiple conformations. The time resolved cryo-EM experiment performed here with the MutS protein demonstrate that the Puffalot can be used in combination with stopped flow kinetic studies that look at protein conformational changes in the millisecond time scale.

Grid preparation using the Puffalot is consistent and reliable, and we believe that it is a useful tool to improve the efficiency of the grid preparation process. Particularly, it can be used to tackle samples that suffer from classical plunge freezing procedures, together with the possibility to perform time-resolved cryo-EM.

Material And Methods

Protein samples

Human ApoF was expressed in *E. coli* BL21 (DE3) (Novagen) at 20 ⁰C overnight. Cell pellets were lysed by sonication and clarified by centrifugation at 24000 x g. Protein purification was performed using a HisTrap column pre-equilibrated in 20 mM Imidazole, 50 mM Tris pH 7.5, 500 mM NaCl, 2 mM DTT and eluted using a gradient of the same buffer containing 500 mM Imidazole. The his-tag was removed by digestion with *3C protease* overnight at 4 ⁰C, followed by a size exclusion column equilibrated with 20mM Tris pH 8.0, 150mM NaCl and 2mM DTT. *Escherichia coli* Polymerase I was expressed in *E. coli* BL21 (DE3) (Novagen) for two hours at 30 ⁰C. Cell pellets were lysed by sonication and clarified by centrifugation at 24000 x g. Protein purification was performed using a HisTrap column pre-equilibrated in buffer 25 mM Imidazole pH 7.5, 500 mM NaCl, 2mM DTT, 5% Glycerol and eluted using a gradient of the same buffer containing 500 mM Imidazole. The his-tag was removed by overnight digestion, followed by a second Histrap column to remove undigested protein. The flowthrough was injected onto a Hitrap Q column pre-equilibrated in buffer 25mM Tris pH 8.0, 2 mM DTT, 10% Glycerol with 150 mM NaCl and eluted with a gradient of the same buffer containing 1M NaCl. *Escherichia coli* MutS was expressed and purified as in [21]. β-galactosidase from *Thermotoga maritima* was expressed and purified as in S. M. Amil *et al.* [22].

Cryo-EM grid preparation

For Puffalot grid preparation, Cu R0.6/1 holey carbon grids (Quantifoil) were glow discharged at 25 mA for 5 s using the Emitech K950 apparatus (Quorum). For all datasets except the time resolved MutS experiment, 6 μL of sample at 4 uM were applied on the grid using the automated injection through Hamilton syringe. For the time resolved MutS experiment, one syringe was filled with MutS protein solution at 8 uM and the second syringe was filled with ATP solution at 6 mM. Mixing of MutS and ATP in 1:1 ratio was obtained on the grid. The solenoids impulse that injects the sample on the grid was set to

50 ms. The excess of buffer is removed by a puff of nitrogen gas at 7 bar for 50 or 100 ms. After the buffer is removed the grids are plunged into a temperature controlled ethane bath at ~-182 °C. The descending time was measured to be of ~30 ms. was For Leica GP2 grids preparation, 3 μl of protein sample was adsorbed onto glow-discharged Cu R0.6/1 holey carbon grid, blotted for 1 s at 80% humidity at 4 °C and flash-frozen in liquid ethane.

SPA data collection

The Apoferritin, Polymerase I - DNA and time resolved MutS plus ATP datasets were collected at the Netherlands Center for Electron Nanoscopy (NeCEN) using a Titan Krios operated at 300 kV. All other datasets were collected at Leiden University Medical Centre (LUMC) using a Talos Arctica operated at 200 kV. Both microscopes were equipped with a K3 direct electron detector and a Bioquantum energy filter (Gatan). The slit width of the energy filter was set to 20 eV. Images were recorded with EPU software (Thermo Fisher Scientific) in super resolution counting mode. Dose, magnification and effective pixel size are detailed in Table 1.

SPA data processing

All image processing was done using Relion 4.0 [23] . Pre-processing and auto-picking were performed with analogous procedures among all datasets. The images were drift corrected using Relion's own (CPU-based) implementation of the UCSF motioncor2 program, and defocus was estimated using CTFFIND4.1 [24]. LoG-based or topaz auto-picking was performed on a subset of micrographs, and picked particles were 2D classified. Selected classes from the 2D classification were used as references for topaz training which was followed auto-picking on the whole dataset.

Apoferritin processing: Extraction box size was set to 540 pixels and binned to 270 pixels (1.312 Å/pix). After one round of 2D classification, good classes were selected for initial model generation in Relion. The initial model was used as reference for 3D classification into different classes. The selected classes from 3D classification were subjected to 3D auto refinement followed by Bayesian polishing. Polished particles were used for 3D classification. Selected particles were subjected to a 3D auto-refine job followed by to one round of CTF (magnification, beam tilt and defocus) refinement and a final Bayesian polishing with parallel rescaling of the box size to 540 pixels (0.656 Å/pix). After a second round of CTF refinement (magnification, beam tilt and defocus) the 3D auto refine job yielded a final map with a nominal resolution of 1.8 Å.

MutS time resolved processing: Extraction box size was set to 512 pixels and binned to 256 pixels (1.672 Å/pix). After one round of 2D classification, good classes were 3D classified using a previously solved structure (PDB: 7OTO [21]) as an initial model. Selected classes from 3D classification were used for Bayesian polishing followed by another round

of 3D classification. Two different classes from the last 3D classification job were selected individually and used for further processing.

MutS preferred orientation processing: Extraction box size was set to 256 pixels and binned to 128 pixels (1.672 Å/pix). After one round of 2D classification, good classes were 3D classified using a previously solved structure (PDB: 7OU2 [21]) as an initial model. Selected class from 3D classification was used for Bayesian polishing followed by CTF refinement (magnification, beam tilt and defocus). A final number of 22k particles was randomly selected and used for a final 3D auto refine job, which was used to assess the angular distribution of individual particles.

β-galactosidase processing: Identical processing pipeline was performed on data coming from Puffalot grid and from Leica grid. Extraction box size was set to 434 pixels and binned to 128 pixels (3.52 Å/pix). After one round of 2D classification, good classes were used for automated initial 3D model generation in Relion followed by 3D classification. Best 3D class was selected, and used for 3D auto refine job applying D4 symmetry. A final number of 1400 particles was randomly selected and used for a final 3D auto refine job, which was used to assess the angular distribution of individual particles.

Tomography data collection and analysis

Tomograms were collected at the Netherlands Center for Electron Nanoscopy (NeCEN) using a Titan Krios operated at 300 keV. Images were recorded with Tomo 5 software (Thermo Fisher Scientific), and collected using a Falcon 3 detector. The detector was used in linear mode at a nominal magnification of 49,000× for a pixel size of 3.097 Å at the sample. Tomographic tilt series were collected from ± 50° in 2° increments with a dose rate of 1.2 electrons per $Å^2$ per sec for a total dose of 70 electrons per $Å^2$. Tomograms were reconstructed from raw tilt series using IMOD (version 4.11.13) [25] using SIRT like function. Tilt series did not contain fiducials markers hence we used patch tracking to align. Ice thickness and all other analysis were also done in IMOD.

Table 1 | Cryo-EM data acquisition parameters

	apoF	β-galactosidase	MutS (orientation)	MutS (time-resolved)
Data collection and processing				
Magnification	130,000	79,000	79,000	105,000
Voltage (kV)	300	200	200	300
Electron exposure (e–/Å^2)	40	50	50	50
Defocus range (μm)	0.5 to 1.8	0.5 to 1.8	0.8 to 2	0.5 to 2
Pixel size (Å)	0.656	1.08	1.08	0.836
Energy filter slit	20 eV	20 eV	20 eV	20 eV
Initial particle images (no.)	800000	4600	100000	
Final particle images (no.)	219000	1408	22000	
Map resolution (Å)	1.8	8.68	3.4	3.8
FSC threshold	1.43	1.43	1.43	1.43

Supplementary material
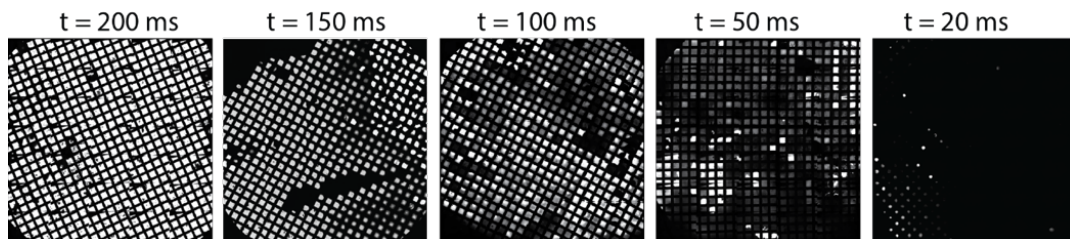
Supplementary Figure 1 | Effect of different "puff" times on ice-thickness. From left to right, decreasing "puff" times show gradients of overall ice thickness on the grid surface.

Supplementary Figure 1

Mean squared distance calculations

In order to calculate the mean distance that a protein of average radius (100 Å to 500 Å) travel in a time range of 10 ms to 1 s, this formula can be used.

$$\langle d \rangle = \sqrt[2]{q \times t \times D}$$

Where:

- $\langle d \rangle$ is the mean distance (μm)
- q is a dimension factor, that is 2, 4 or 6 depending upon whether diffusion occurs in 1, 2, or 3 dimensions, respectively;
- t is time (s)
- D is the diffusion constant that depends on the radius of the particle, the viscosity of the solution and on the temperature. For a protein of average radius (100 Å to 500 Å) in aqueous solution at 4°C, D varies from ~4 to 20 ($^{\mu m^2}/_s$) .

Here is the calculations based on a protein of radius 100 Å, at 4°C in aqueous solution (D=20), travelling in one dimension (i.e. from top to bottom air-water interface surfaces) in 10 ms or 1000 ms:

$$\langle d \rangle_{10\ ms} = \sqrt[2]{2 \times 0.01 \times 20} \cong 0.6\ \mu m$$

$$\langle d \rangle_{1000\ ms} = \sqrt[2]{2 \times 1 \times 20} \cong 6\ \mu m$$

References

1.   Schultz, P. Cryo-electron microscopy of vitrified specimens. *Q. Rev. Biophys.* **21**, 129–228 (1988).

2.   Carragher, B. *et al.* Current outcomes when optimizing 'standard' sample preparation for single-particle cryo-EM. *J. Microsc.* **276**, 39–45 (2019).

3.   Armstrong, M. *et al.* Microscale Fluid Behavior during Cryo-EM Sample Blotting. *Biophys. J.* **118**, 708–719 (2020).

4.   Zi Tan, Y. *et al.* Addressing preferred specimen orientation in single-particle cryo-EMthrough tilting. *Nat. Methods* **14**, 793–796 (2017).

5.   Noble, A. J. *et al.* Reducing effects of particle adsorption to the air–water interface in cryo-EM. *Nat. Methods* **15**, 793–795 (2018).

6.   Meyerson, J. R. *et al.* Self-assembled monolayers improve protein distribution on holey carbon cryo-EM supports. *Sci. Rep.* **4**, 1–5 (2014).

7.   Glaeser, R. M. & Han, B.-G. Opinion: hazards faced by macromolecules when confined to thin aqueous films. *Biophys. Reports* **3**, 1–7 (2017).

8.   Glaeser Robert M. Proteins, interfaces, and cryo-em grids. *Curr. Opin. Colloid Interface Sci.* **25**, 289–313 (2016).

9.   D'Imprima, E. *et al.* Protein denaturation at the air-water interface and how to prevent it. *Elife* **8**, 1–18 (2019).

10.   Arnold, S. A. *et al.* Blotting-free and lossless cryo-electron microscopy grid preparation from nanoliter-sized protein samples and single-cell extracts. *J. Struct. Biol.* **197**, 220–226 (2017).

11.   Ravelli, R. B. G., Nijpels, F. J. T., Henderikx, R. J. M. & Weissenberger, G. Automated cryo - EM sample preparation by pin - printing and jet vitrification. (2019).

12.   Jain, T., Sheehan, P., Crum, J., Carragher, B. & Potter, C. S. Spotiton: A prototype for an integrated inkjet dispense and vitrification system for cryo-TEM. *J. Struct. Biol.* **179**, 68–75 (2012).

13.   Ivan Razinkov, Venkat Dandey, Hui Wei, Zhening Zhang, David Melnekoff, William J. Rice, Christoph Wigge, Clinton S. Potter, and B. C. HHS Public Access. *J Struct Biol* **195**, 190–198 (2016).

14. Feng, X. *et al.* A Fast and Effective Microfluidic Spraying-Plunging Method for High-Resolution Single-Particle Cryo-EM. *Structure* **25**, 663-670.e3 (2017).

15. Rubinstein, J. L. *et al.* Shake-it-off: A simple ultrasonic cryo-EM specimen-preparation device Rubinstein John L. *Acta Crystallogr. Sect. D Struct. Biol.* **75**, 1063–1070 (2019).

16. Kontziampasis, D. *et al.* A cryo-EM grid preparation device for time-resolved structural studies. *IUCrJ* **6**, 1024–1031 (2019).

17. Klebl, D. P., White, H. D., Sobott, F. & Muench, S. P. On-grid and in-flow mixing for time-resolved cryo-EM. *Acta Crystallogr. Sect. D Struct. Biol.* **77**, 1233–1240 (2021).

18. Glaeser, R. M. Preparing Better Samples for Cryo-Electron Microscopy: Biochemical Challenges Do Not End with Isolation and Purification. *Annu. Rev. Biochem.* **90**, 451–474 (2021).

19. Klebl, D. P. *et al.* Need for Speed: Examining Protein Behavior during CryoEM Grid Preparation at Different Timescales. *Structure* **28**, 1238-1248.e4 (2020).

20. Sharma, A., Doucette, C., Biro, F. N. & Hingorani, M. M. Slow conformational changes in MutS and DNA direct ordered transitions between mismatch search, recognition and signaling of DNA repair. *J. Mol. Biol.* **425**, 4192–4205 (2013).

21. Borsellini, A., Kunetsky, V., Friedhoff, P. & Lamers, M. H. Cryo-EM structures reveal how ATP and DNA binding in MutS 3 coordinate the sequential steps of DNA mismatch repair 4 5 6. doi:10.1101/2021.06.03.446775

22. Míguez Amil, S. *et al.* The cryo-EM Structure of Thermotoga maritima β-Galactosidase: Quaternary Structure Guides Protein Engineering. *ACS Chem. Biol.* **15**, 179–188 (2020).

23. Kimanius, D., Dong, L., Sharov, G., Nakane, T. & Scheres, S. H. W. New tools for automated cryo-EM single-particle analysis in RELION-4.0. *Biochem. J.* **478**, 4169–4185 (2021).

24. Rohou, A. & Grigorieff, N. CTFFIND4: Fast and accurate defocus estimation from electron micrographs. *J. Struct. Biol.* **192**, 216–221 (2015).

25. Kremer, J. R., Mastronarde, D. N. & McIntosh, J. R. Computer visualization of three-dimensional image data using IMOD. *J. Struct. Biol.* **116**, 71–76 (1996).